Structural Eng./Earthquake Eng., JSCE, Vol. 14, No. 1, 51s—61s, 1997 April

ELASTO-PLASTIC BEHAVIOR OF STEEL CANTILEVER COLUMNS WITH VARIABLE CROSS-SECTION SUBJECTED TO HORIZONTALLY CYCLIC LOAD

Toshihiro MIKI

Member of JSCE, Dr. of Eng., Associate Professor, Dept. of Civil Eng., Daido Institute of Technology
(40 Hakusui-cho Minami-ku Nagoya 457 Japan)

This paper deals with the elasto-plastic behavior of cantilever columns with variable cross-section subjected to horizontally cyclic load. The numerical results based on the plastic zone theory show that the different collapse modes may appear in such columns every half cycle. This phenomenon occurs due to the presence of two or more collapse mechanisms as well as the combined action of vertical load and accumulated residual deformation of column by cyclic bending. This behavior can be classified as an instability phenomenon of columns under cyclic loading which cannot be predicted through the overall buckling and bending strengths of columns.

Key Words : *variable cross-section, column, hysteresis loop, elasto-plastic analysis, rigid plastic mechanism*

1. INTRODUCTION

Steel framed structures such as bridge piers and pylons have generally been composed of variable cross-section members[1]. In most cases, the cross-sectional and material properties change abruptly in the longitudinal directions of frame members. The variable cross-section has been designed on the basis of the rational design concept to utilize as fully as possible the potential capacity of given materials. However, very little is known about the effects of variable cross-section on the earthquake resistance of frames.

For steel columns and frames with uniform cross-section which are subjected to horizontal cyclic loading, the fundamental inelastic behavior can be summarized as follows[2)-5)]; i) the hysteresis loops of frames made of low yield mild steel approach the upper bound mechanism line obtained by assuming zero thrust force in the second order rigid plastic analysis, ii) frames made of high tensile strength steel would not always have the corresponding capacity, and iii) the decrease in load carrying capacities of frames are almost caused by local and torsional bucklings. In addition, Nakamura and Uetani[6)] have pointed out the other factor except local and torsional bucklings for the decrease in strength of cantilever columns.

In the case of columns with variable cross-section, the resistance bending moment distributes similar to the induced one with distance along the columns. Then plastic deformation may occur near the location of change in cross-section as well as column base and beam-to-column connections. Such inelastic behavior must be greatly different from the one of columns with uniform cross-section.

This paper studies the elasto-plastic behavior of columns with variable cross-section subjected to horizontally cyclic load under the constant vertical load. Firstly, the numerical method for columns is briefly described by using the plastic zone theory[7)] and arc length method[8)]. Secondly, the collapse modes of columns are investigated by means of the second order rigid plastic analysis. Through the numerical results, the inelastic hysteretic behavior of columns with variable cross-section is discussed in detail by focusing on the collapse modes, strain and energy absorption of each cross-section and restoring force. Finally, the variation of collapse modes with the location of change in cross-section demonstrates

This paper is translated into English from the Japanese paper, which originally appeared on J. Struct. Mech. Earthquake Eng., JSCE, No.446/I-19, pp.127 -136, 1992.4.

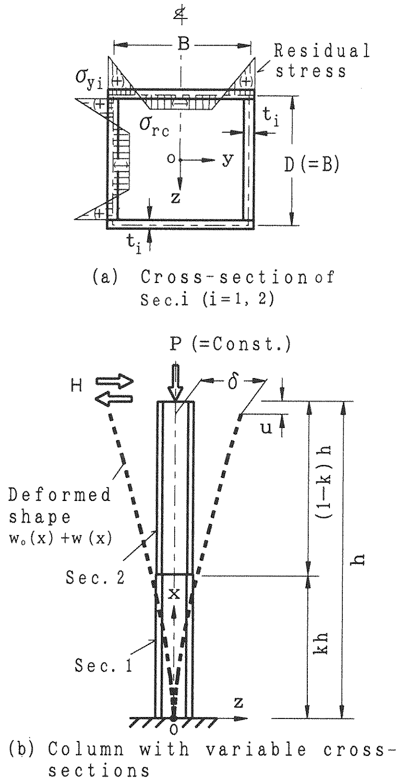

Fig.1 Column subjected to cyclic load H

the transition region of the instability phenomenon peculiar to variable cross-section .

2. ELASTO-PLASTIC ANALYSIS PROCEDURE OF COLUMNS WITH VARIABLE CROSS-SECTION

(1) Numerical model of columns with variable cross-section

There are many factors which influence upon the elasto-plastic hysteretic behavior of columns with variable cross-section i.e., the number of cross-sections, the location of change in cross-section, combination of cross-sectional and material properties, column slenderness, initial imperfection, magnitude of vertical load and cyclic loading condition.

By considering these factors, the attention is paid to the cantilever columns consisting of two portions, Sec.1 and Sec.2, in **Fig.1**. Sec.1 and Sec.2 have the same dimensions, B and D, and yield stress σ_y but the plate thickness t_1 is larger than t_2, so that the cross-sectional properties change abruptly at the location of $x=kh$. Vertical load P is kept constant while horizontal load H is applied at the top of columns.

Table 1 Dimension and properties of cross-section

Items / Sec.i	B(=D) (mm)	t_i (mm)	A_i (cm²)	I_i (×10⁵cm⁴)	σ_{yi} (MPa)	N_{yi} (KN)	M_{pi} (KN·m)
1	750	33	990	9.2992	314	31,069	8,744
2	750	22	660	6.1928	314	20,713	5,827

Notes: A_i: Cross-sectional area, I_i: Moment of inertia, σ_{yi}: Yield point, N_{yi}: Squash force, and M_{pi}: Fully-plastic moment.

Referring to the imperfection tolerance for compressive columns provided by Japanese Highway Specification[9], an initial imperfection in the columns is assumed of the form

$$w_o(x) = \frac{h}{1{,}000}\left(\frac{x}{h} - \sin\frac{\pi x}{h}\right) \tag{1}$$

The residual stress distribution adopted in the analysis is shown in **Fig.1**(a). The maximum compressive residual stress is taken as 0.4 times σ_y.

When performing the numerical analysis, the columns are divided into thirty elements with the same length so as to follow the sway displacement modes of columns as exactly as possible.

Table 1 gives the cross-sectional dimensions and properties of Sec.1 and Sec.2. The columns C0-C12 used in analysis are listed in **Table 2** as parameters of column height (h=9m and 12 m), location of change in cross-section (k=0 to 0.6), existence of initial imperfection, and squash force ratio P/N_{y2} (=0.3 and 0.5) of vertical load P to squash force N_{y2} of Sec.2.

These columns were designed by considering which of sections, Sec.1 or Sec.2, reaches yield or fully-plastic state first. **Table 2** includes the horizontal load H_y corresponding to initial yield of columns and the plastic hinge loads, H_{p1}, H_{p2}, H_{u1} and H_{u2}, which mean the points of intersection between a linear elastic solution and plastic collapse mechanism lines as explained later. $\bar{\lambda}_y$ is the reference value of column slenderness, which is obtained by correlating the inelastic buckling strength of variable cross-section columns with that of columns with uniform cross-section, Sec.2, on the SSRC column strength curve II[10]

The columns in **Table 2** are denoted by the following expression;

C1 W R - 0.4 - 0.7
- e) Column slenderness $\bar{\lambda}_y$
- d) Ratio of length in Sec.1 to column height h
- c) R: with residual stress
- b) W: with initial deflection
- a) No. of analytical model

For a more convenient treatment for discussion,

Table 2 List of columns with variable cross-section analyzed in this paper

Items / Column	h (m)	k	$\bar{\lambda}_y$	$\frac{P}{N_{y2}}$	$\frac{P_u}{N_{y2}}$	δ_y/h	H_y (KN)	H_{p1} (KN)	H_{p2} (KN)	H_{pu1} (KN)	H_{pu2} (KN)	$\frac{H_{pm}}{H_y}$	$\frac{H_{pum}}{H_y}$
C0 - 0 -0.72	9.0	0	0.72	0.5	0.777	0.00592	279.7(S1)	—	353.9	—	531.0	—	1.898
C1 -0.4-0.49 C2W -0.4-0.49 C3WR-0.4-0.49	9.0	0.4	0.49	0.5	0.883	0.00728	466.2(S2)	712.4	566.4	836.2	849.9	1.215	1.794
C4WR-0.2-0.61	9.0	0.2	0.61	0.5	0.831	0.00620	349.6(S2)	699.4	438.8	820.9	658.3	1.355	1.883
C5WR-0.3-0.55		0.3	0.55		0.857	0.00603	399.6(S2)	706.7	495.4	829.6	743.2	1.239	1.860
C6WR-0.4-0.49		0.4	0.49		0.883	0.00728	466.2(S2)	712.4	566.4	836.2	849.9	1.215	1.794
C7WR-0.5-0.43		0.5	0.43		0.907	0.00827	552.2(S1)	716.5	658.7	841.0	988.3	1.193	1.523
C8WR-0.6-0.37		0.6	0.37		0.930	0.00803	552.2(S1)	719.3	783.6	844.3	1,175.7	1.302	1.529
C9WR-0.2-0.88	12.0	0.2	0.88	0.3	0.685	0.01542	367.1(S2)	576.9	429.2	609.4	487.7	1.169	1.329
C10WR-0.3-0.82		0.3	0.82		0.719	0.01643	419.6(S2)	583.3	484.2	616.2	550.0	1.154	1.311
C11WR-0.4-0.76		0.4	0.76		0.755	0.01813	489.5(S2)	588.3	553.1	621.4	628.5	1.299	1.269
C12WR-0.5-0.68		0.5	0.68		0.796	0.01765	497.0(S1)	591.9	642.1	625.2	729.7	1.191	1.258

Notes; 1)h and k: See Fig.1(b). 2) $\bar{\lambda}_y$: Column slenderness on the basis of Sec.2. 3)P_u: Overallbuckling strength of columns with initial imperfections ($w_o(h)=0.001h$ and $\sigma_{rc}=-0.4\sigma_y$) under the condition of $E_t=0.01E$. 4)N_{y2}: Squash force of Sec.2 (See Table 1). 5)H_y and δ_y: Horizontal load and sway displacement, respectively, corresponding to initial yield (See Fig.4). 6) (S1) and (S2) mean that initial yield occurs at the location of Sec.1(X=0) and Sec.2(x=kh), respectively. 7)H_{p1}, H_{p2}, H_{pu1} and H_{pu2}: See Fig.4. 8)H_{pm}=Min.{H_{p1},H_{p2}}. 9)H_{pum}=Min.{H_{pu1}, H_{pu2}}.

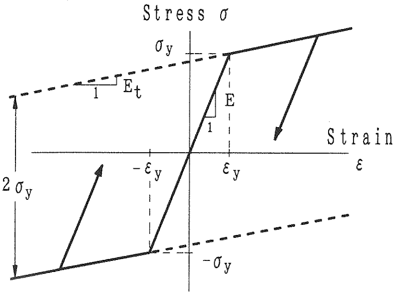

Fig.2 Stress - strain relationship

the columns are specified by the notation a) or a)b)c).

(2) Numerical procedure for columns under cyclic loading

In the numerical analysis, the geometrical and material nonlinearities of columns are taken into account by the updated-Lagrangian method and plastic zone theory[7)], respectively. A subroutine program for applying the arc length control method[8)] is added to the software presented before[7)]. In order to perform the elasto-plastic hysteretic analysis of columns, the following points are modified.

a) Stress - strain relationship

Fig.2 shows the bi-linear type of stress - strain relationship[5)] used in the analysis. E is Young's modulus (=2.1×10^5 Mpa). E_t is strain hardening modulus and will be explained in the numerical results. The cross-section is divided into small segments to consider the propagation of plastic zone. The tangent modulus varying linearly is assumed in a small segment[7)].

b) Solution algorithm for nonlinear analysis

The solution algorithm for nonlinear analysis is based on the arc length control method[8)] which can automatically go through the limit points of loads as well as displacements. This method is a powerful nonlinear analytical technique for a parameter of an arc length on the equilibrium path, but has the difficulty to directly control the displacement of a specified point like the displacement control method.

In this paper, a conventional procedure for judging the displacement reversal is described for the hysteretic analysis of columns under alternating sway displacement amplitude at the top of the column.

Firstly, when nonlinear calculation goes forward from a certain equilibrium state i to the next state i+1, the displacement δ_{i+1} at a specified point for the state i+1 is approximated by

$$\delta_{i+1} = \delta_i + (\delta_i - \delta_{i-1})\frac{\Delta l_{i+1}}{\Delta l_i} \tag{2}$$

where δ_i = displacement at the state i, Δl_i = incremental arc length used in the state i-1 to i, and Δl_{i+1}= incremental arc length assumed in the state i to i+1 according to Ref.8).

Secondly, $|\delta_{i+1}|$ is compared with the maximum displacement amplitude δ_m which is given as an input datum. If $|\delta_{i+1}|$ is larger than $|\delta_m|$, Δl_{i+1} has to be modified by

$$\Delta l_{i+1} = \Delta l_i \frac{|\delta_m - \delta_i|}{|\delta_{i+1} - \delta_i|} \tag{3}$$

In the case of $|\delta_{i+1}|\le|\delta_m|$, of course, the calculation is proceeded without modifying the arc length Δl_{i+1}.

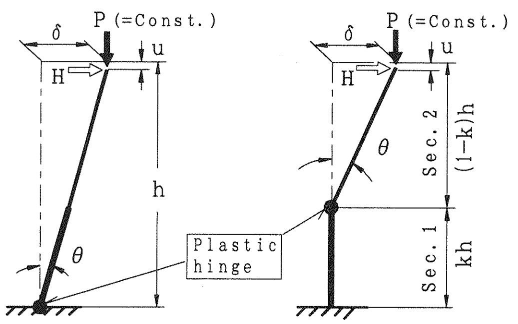

(a) Mode V (V_u) (b) Mode Y (Y_u)

Fig.3 Plastic collapse mechanism of columns with variable cross-section

When the difference between the numerical response δ_{i+1} corresponding to Δl_{i+1} and δ_m is less than 0.01%, the sign of load vector is changed in order to give the displacement reversal at the specified point in the column.

3. RIGID PLASTIC AND ELASTO-PLASTIC ANALYSES OF COLUMNS SUBJECTED TO MONOTONIC LOADING

(1) Rigid plastic analysis of columns with variable cross-section

For comparison purposes, the second order rigid plastic analysis is performed for columns with variable cross-section subjected to increasing horizontal load H and constant vertical load P.

For the columns with two cross-sections, the plastic moment changes abruptly at the location of change in cross-section. Then, as shown in **Fig.3**, there exist two plastic collapse mechanisms, V and Y, in which the plastic hinges are assumed at the bottoms of Sec.1 and Sec.2, respectively. These mechanisms are also thereafter referred to as collapse modes.

a) Plastic mechanism line of mode V (See **Fig.3(a)**)

The equilibrium of external and internal work in mode V leads to an equation relating the vertical load P, horizontal load H, sway displacement δ, vertical displacement u and rotational angle θ, which is given by

$$H\delta + Pu = M_{pn1}\theta \tag{4}$$

Seeing the geometrical form of deformed column, the following relationships can be found.

$$\theta \cong \tan\theta = \delta / h, \quad u = \delta \tan\theta \tag{5a,b}$$

Substituting Eq.(5) into Eq.(4), the relationship between H and δ can be obtained as

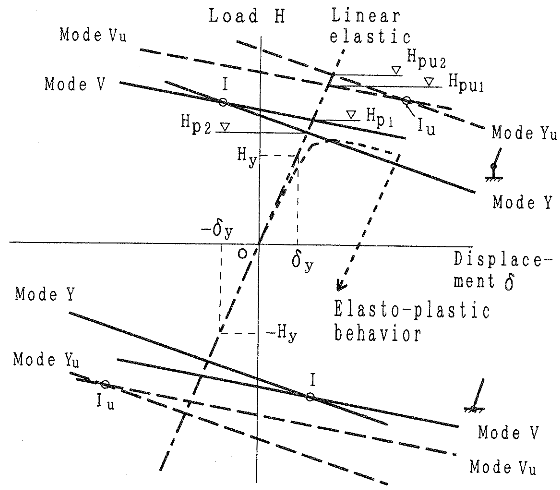

Fig.4 Horizontal load - sway displacement curves predicted by rigid plastic theory

$$H = \frac{M_{pn1}}{h} - \frac{P\delta}{h} \tag{6}$$

b) Plastic mechanism line of mode Y (See Fig.3(b))

In the case of the mode Y, noting that the plastic hinge is formed in Sec.2 at the junction of Sec.1 and Sec.2, H - δ relationship is given by

$$H = \frac{M_{pn2}}{(1-k)h} - \frac{P\delta}{(1-k)h} \tag{7}$$

In Eqs.(4), (6) and (7), M_{pni} is the reduced plastic moment of Sec.i depending on the magnitude of vertical load P.

c) Upper bound mechanism lines of modes V and Y

Substitution of the fully plastic moment M_{pi} into M_{pni} in Eqs.(6) and (7) gives the upper bound mechanism lines, V_u and Y_u, which have the same slopes as V and Y, respectively. These are helpful to understanding the variation of hysteresis loops[3)] due to strain hardening discussed later.

d) Variation of collapse mechanism lines

As illustrated in **Fig.4**, the column with variable cross-section under consideration has four mechanism lines given by Eqs.(6) and (7) in the H - δ plane. In this figure, $I(I_u)$ is the crossing point of $Y(Y_u)$ and $V(V_u)$, and means the instability point where the plastic hinges are formed in Sec.1 and Sec.2 at the same time. The negative slope of lines Y and Y_u becomes significant with an upward movement of the junction between cross-sections and an increase in vertical load P. Clearly, for the columns with uniform cross-section, Y and Y_u are coincident with V and V_u, respectively.

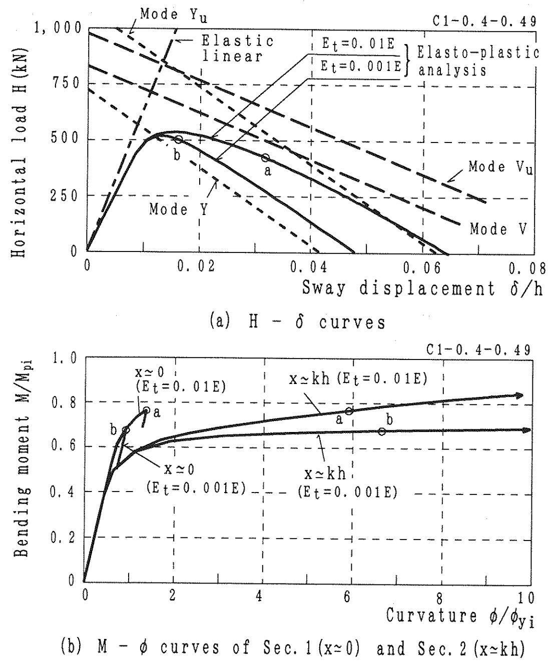

Fig.5 Monotonic analysis of columns with variable cross-section (P=0.5N_{y2})

(2) Elasto-plastic analysis of columns with variable cross-section

The elasto-plastic behavior and collapse modes of columns with k of 0.4 are investigated under the condition of monotonic loading. E_t is set as 0.001E or 0.01E.

Fig.5 shows the load H - displacement δ curves and bending moment M - curvature ϕ curves of Sec.1 at $x \cong 0$ and Sec.2 at $x \cong kh$, in which M and ϕ are non-dimensionalized by the fully-plastic bending moment M_{pi} and yield curvature ϕ_{yi} (=2$\sigma_y/E/(D+t_i)$) of Sec.i. The points a and b plotted on H - δ curves correspond to those on M - ϕ curves.

The slope of H - δ curve for E_t/E=0.001 after the maximum load is almost equal to that of mode Y. While the corresponding slope for E_t/E=0.01 becomes significant with an increase in δ through the point a.

As shown in the M - ϕ curves, unloading appears near the column base at the points a and b regardless of the E_t/E value. This result provides evidence that the collapse modes vary from V to Y over the maximum load points on H - δ curves in spite of the loading being monotonic. This phenomenon is due to $P\Delta$ moment caused by the combined action of vertical load P and increasing sway displacement δ. In other words, with an increase in δ, the internal plastic work in mode Y decreases and the one in V increases.

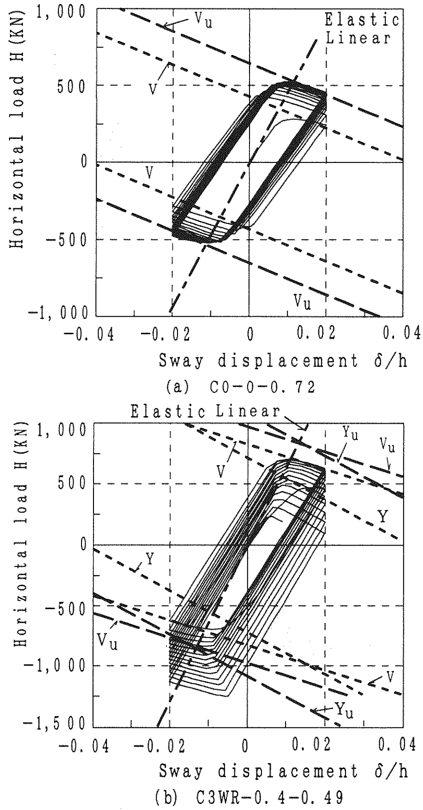

Fig.6 Load - displacement curves of columns C0 and C3WR (E_t=0.01E, P=0.5N_{y2})

It should be noted that such elasto-plastic behavior is peculiar to the columns with variable cross-section which have at least two collapse modes.

4. ELASTO-PLASTIC HYSTERETIC BEHAVIOR OF COLUMNS WITH VARIABLE CROSS-SECTION

The columns, C0 and C1-C3, with uniform cross-section and variable cross-section (k=0.4), respectively, were analyzed under horizontal cyclic loading with P/N_{y2}=0.5. Cyclic loading is accomplished by the control of constant tip displacement $\delta_m = \pm 0.02h$. This value corresponds to 3.8δ_y and 2.8δ_y for columns, C0 and C1-C3, respectively, in which δ_y is initial yield displacement (See **Table 2**). Only the column C1 with E_t of 0.001E is analyzed between δ_m=0.025h and -0.0125h because of the difficulty of solution convergence.

(1) Relationships between horizontal load H and sway displacement δ at the top of column

Fig.6 compares H - δ curves of the column C0

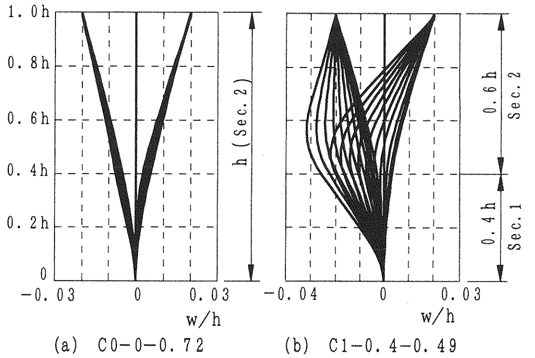

Fig.7 Sway displacement modes of columns (E_t=0.01E, P=0.5N_{y2})

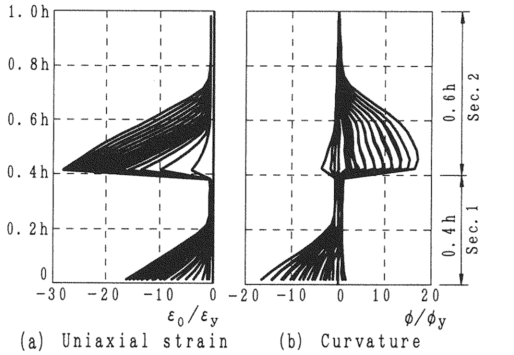

Fig.8 Distribution of uniaxial strain and curvature in column C1-0.4-0.49 ((P=0.5N_{y2}, E_t=0.01E)

with that of C3WR.

a) Column with uniform cross-section C0-0-0.72 (E_t=0.01E, See Fig.6(a))

For increasing number of cycles, the hysteresis H - δ loops expand with the centre of origin and become asymptotic to the upper bound collapse mode V_u as already pointed out by Igarashi[3] et al. This result implies that a typical elasto-plastic behavior[3] of columns made of mild steel can be realized by assuming E_t=0.01E in the bi-linear type of stress-strain relationship.

b) Column with variable cross-section C3WR-0.4-0.49 (E_t=0.01E, **Fig.6**(b))

In the positive region of load H, H-δ curve extend up to the mechanism line V in a few cycles and the slope between the peak load and displacement reversal in each loop is almost equal to that of mode V. For increasing number of cycles, however, the peak loads decrease and corresponding slopes become close to the line Y.

On the other hand, in the negative region of H, the slope after peak loads equals that of mechanism line V for each hysteresis loop. The resistance load then rises more and more with an increase in cycle number. This behavior is opposite to that in the positive region of H.

It can therefore be predicted that the column C3 shows an interesting elasto-plastic behavior, in which two different collapse modes appear in one hysteresis loop. Such behavior was also observed in H - δ curves of columns C1 and C2W.

(2) Sway displacement modes of columns

Fig.7 compares the sway displacement modes at the displacement reversals for columns C0 and C1 with uniform cross-section and variable cross-section, respectively. E_t is taken as 0.01E in the analysis.

The displacement mode of column C0 is almost symmetrical for positive and negative tip displacements. On the contrary, the column C3 bends remarkably at the middle of column and is S shaped as if the modes V and Y would be combined.

Nakamura and Uetani[6] have found a weakening phenomenon for cantilever column with uniform cross-section subjected to horizontally cyclic load. This phenomenon results from the propagation and accumulation of plastic deformation for increasing number of cycles leading to a new collapse mechanism. This causes S shaped displacement modes similar to those shown in **Fig.7**(b). Furthermore, developing the symmetry limit theory with respect to displacement modes, a symmetry limit curve is proposed for design use as functions of squash force ratio, column slenderness and tip displacement. According to this proposal, the column C0 is just on the boundary of symmetrical and antisymmetrical modes. As can be seen from **Fig.7**(a), this column shows slight antisymmetric behavior.

(3) Strain distribution in columns

Fig.8 shows the variation of uniaxial strain ε_o and curvature ϕ with distance along the column C1 (E_t=0.01E) at the reversals of sway displacement δ.

For increasing number of cycles, the uniaxial strain develops extensively from the bottoms of Sec.1 and Sec.2 at the same time. The curvature in Sec.1 is of opposite sign to that of Sec.2 and the location with maximum curvature in Sec.2 then gradually moves up the column[6].

(4) Variation of rotational angle and residual deformation in columns

Fig.9 shows the variations of rotational angles of column C1 with cycle number N, in which R, R_1 and R_2 correspond to the whole of column and portions of

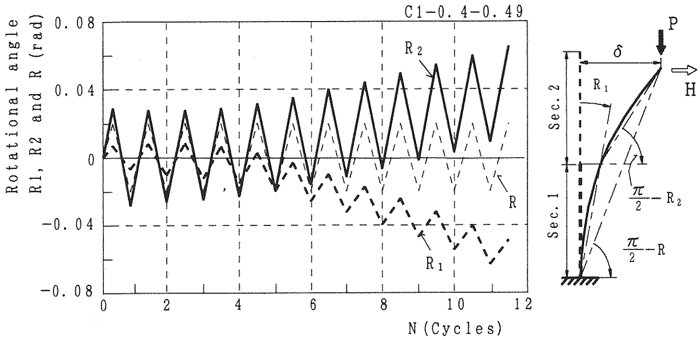

Fig.9 Variation of rotational angle of columns with number of cycles

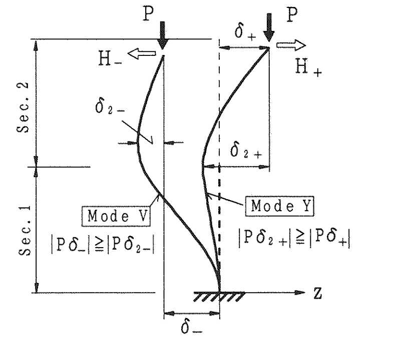

Fig.10 S shaped displacement modes of column with variable cross-section

Sec.1 and Sec.2, respectively. The initial value of N is set as 0.5 cycle at the first displacement reversal and the number of cycles from one reversal to the next is counted as 0.5 cycle.

In the range of N>2.5, R_1 and R_2 begin to vary in the negative and positive directions, respectively. These results are equivalent to the occurrence of S shaped displacement mode. This may be the reason why the difference between the normal strains within the compression and tension sides of cross-section generates residual bending deformation at the displacement reversals.

Referring to **Fig.5**, Sec.2 in the column C1 deforms significantly in the inelastic region when δ=0.02h corresponding to N=0.5. This plastic deformation is retained as the residual deformation with R_2>0 on the way to N=1. As a result, the residual deformation with R_2<0 at N=1 is small or cancels with that when R_2>0 in N=0.5. Furthermore, since the uniaxial strain develops up the column as shown in **Fig.8**(a), the residual deformation appears over a considerable length of the column.

To elaborate on this point, the change of sway displacement modes is illustrated in **Fig.10**. From this figure, the displacement modes with R_1<0 and R_2>0 can be explained as follows;

i) Stage *I*: Compared with the case of no residual deformation, greater $P\Delta$ moment applies at the junction between cross-sections and makes the plastic zone propagate further (mode Y, R_2>0).

ii) Stage *J*: $P\Delta$ moment at the location of change in cross-section declines due to the residual deformation at Stage *I*. Whilst, the plastic deformation develops more at the bottom of Sec.1 (mode V). The residual deformation with R_1<0 then appears.

iii) Stage *K*: The same $P\Delta$ moment described in Stage *I* increases significantly and the plastic deformation begins to concentrate only near the bottom of Sec.2 (mode Y).

iv) Stage *L*: As explained in Stage *J*, the residual deformation with R_1<0 becomes larger due to the plastic deformation at the bottom of Sec.1. At the same time, $P\Delta$ moment (=$P\delta_{2-}$) which gives R_2>0 makes the middle of column bend more.

It is therefore clear that S shaped displacement modes are caused by the variation of $P\Delta$ moment at each cross-section with accumulated residual deformation.

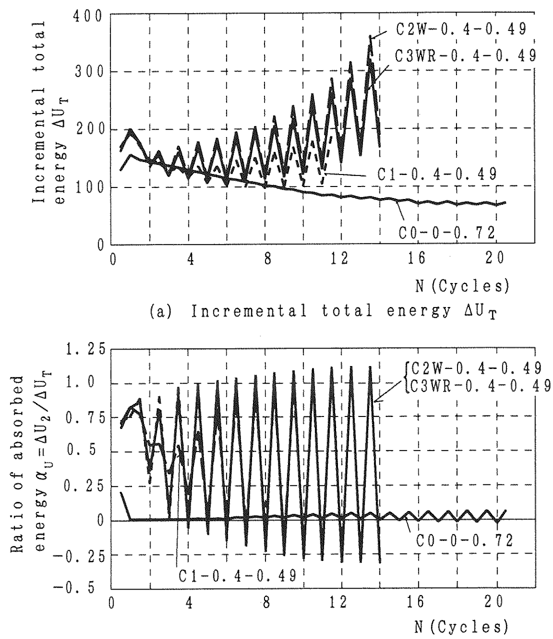

(a) Incremental total energy ΔU_T

(b) Incremental absorbed energy ΔU_2 (x=0. 4h~h)

Fig.11 Variation of incremental absorbed energy with number of cycles (E_t=0.01E, P=0.5N_{y2})

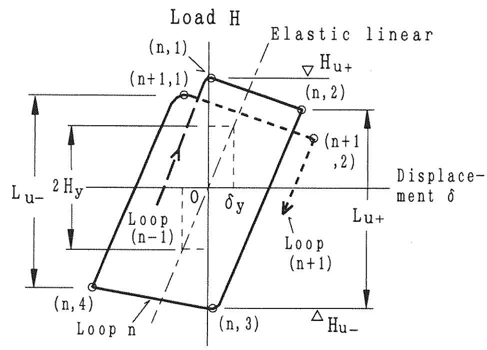

Fig.12 n-th hysteresis loop of load - displacement curve of columns with S shaped displacement modes

(5) Variation of strain energy absorbed by each cross-section

Two incremental absorbed energies of columns were investigated to check the results discussed previously. One is the total strain energy ΔU_T of the column and the other ΔU_2 is the strain energy absorbed by cross-section Sec.2 within the range $0.4h \le x \le 0.6h$. ΔU_2 is rearranged as the ratio to ΔU_T by

$$\alpha_U = \Delta U_2 / \Delta U_T \tag{8}$$

Fig.11 shows the variations of ΔU_T and α_U of columns C0-C3 (E_t=0.01E) with cycle number N.

As is seen from **Fig.11**(a), ΔU_T of the column C0 with uniform cross-section declines gradually and tends to approach a constant value with an increase in N. On the other hand, ΔU_T of columns C1-C3 with variable cross-section decreases and increases every half cycle when $N \ge 2$. This is significant in columns C2 and C3 and can be accounted for by the initial deflection assumed in the same direction as the residual curvature. **Fig.11**(b) also shows that α_U of columns C1-C3 varies severely every half cycle when $N \ge 2.5$.

From these results, there is no doubt that the portion of plastic deformation moves alternately and the two different collapse modes V and Y appear in one hysteresis loop.

(6) Variation of parameters α_H and α_L related to restoring force characteristics of columns

To investigate the restoring force characteristics which measure the inelastic performance of columns, the following two parameters are defined, referring to the n-th hysteresis loop of points (n,1), (n,2)・・・(n+1,1) in **Fig.12**.

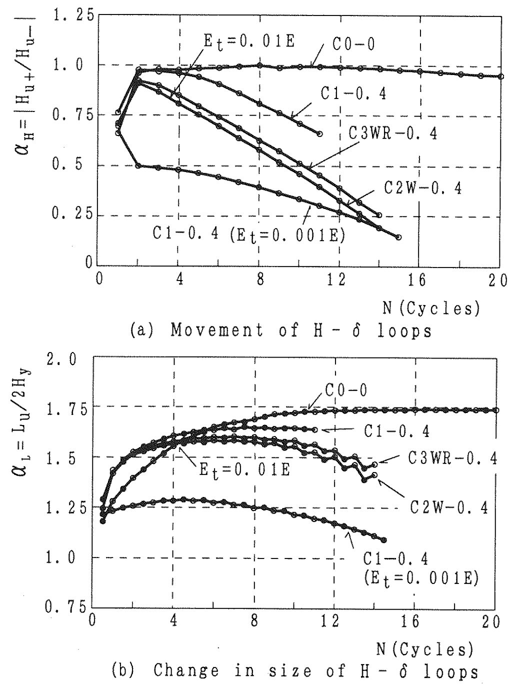

Fig.13 Variation of restoring force quantities α_H and α_L with number of cycles (P=0.5N_{y2})

$$\alpha_H = \frac{|H_{u+}|}{|H_{u-}|}, \quad \alpha_L = \frac{L_{u+}}{2H_y} \quad or \quad \frac{L_{u-}}{2H_y} \tag{9a,b}$$

where L_{u+} and L_{u-} denote the distances from the peak load points (n,3) and (n+1,1) to the reversal points (n,2) and (n,4), respectively. These should be referred to as L_u. H_{u+} and H_{u-} are the peak loads at points (n,1) and (n,3) in the positive and negative regions of load H, respectively. α_H and α_L therefore express the movement of hysteresis loops relative to load H and the increasing and decreasing size of hysteresis loops relative to initial yield load H_y, respectively.

Fig.13 indicates the variations of α_H and α_L of columns C0-C3 (E_t=0.01E) with cycle number N.

a) Movement of hysteresis loops (Fig.13(a))

In the case of column C0 with uniform cross-section, α_H was almost constant at 1.0 for N>2 and hence the absolute values of the peak loads in each hysteresis loop are also almost constant (See **Fig.6**(a)). On the contrary, in the case of columns C1-C3 with variable cross-section, α_H decreases rapidly for N>2 and hence the hysteresis loops move in the direction of negative H. This is predominant for the columns C2 and C3 when there are initial imperfections.

b) Change in size of hysteresis loops (Fig.13(b))

For column C0 with uniform cross-section, α_L increases steadily with an increase in N and ap-

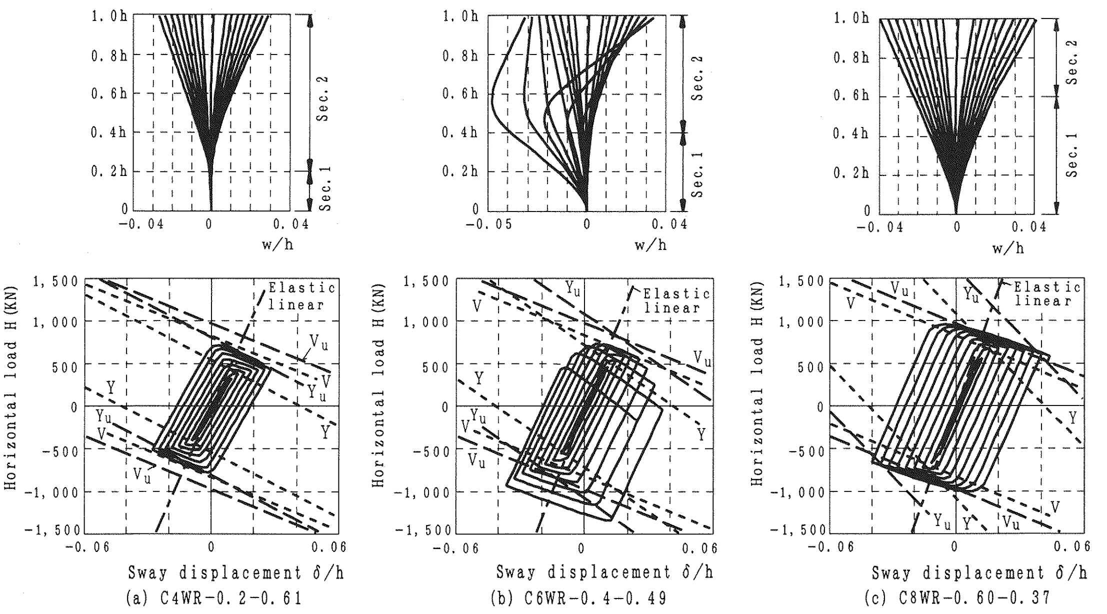

Fig.14 Sway displacement modes and load - displacement curves of columns with variable cross-section (P=0.5N_{y2}, E_t=0.01E)

proaches 1.75 for N≥12. This value is a little less than a load ratio H_{pum}/H_y (=1.898, See **Table 2**) which is the ratio of the upper bound collapse mode V_u. to the initial yield load H_y. This is the reason why the peak load points on hysteresis loops occur a little inside the mechanism line V_u. The hysteresis loops extend almost up to the line V_u due to strain hardening.

On the other hand, α_L for columns C1-C3 (E_t= 0.01E) with variable cross-section increases for N≤8 and the hysteresis loops spread as for column C0. Then the hysteresis loops keep their magnitude when strain hardening is small, e.g. column C1 with E_t of 0.001E. The maximum value of α_L for columns C2W and C3WR with E_t of 0.01E is about 1.63 and greater than H_{pm}/H_y (=1.215) by about 35% but smaller than H_{pum}/H_y(=1.794) by about 12%.

Moreover, the hysteresis loops of columns C1-C3 (E_t=0.01E) reduce when N>8. This tendency is significant for columns C2W and C3WR. This is because of the differences in the variations of peak loads in the positive and negative regions of H as seen from H - δ curve of column C3 (See **Fig.6**(b)). This may also be related to the elasto-plastic behavior in which $P\Delta$ moments at the bottoms of Sec.1 and Sec.2 lead to S displaced shapes.

The variation of α_L is, as a whole, less marked than that of α_H. When the collapse mode begins to change, hysteresis loops tend to move in the direction of the region where mode V appears. It is clear that these variations of hysteresis loops depend on the collapse modes and strain hardening.

5. COLLAPSE MODES OF COLUMNS WITH VARIABLE CROSS-SECTION AND DISCUSSION

The columns C4-C8 and C9-C12 were analyzed under the condition of E_t=0.01E and P/N_{y2}= 0.3 or 0.5 for different values of k, which denotes the location of change in cross-section. Varying k alters the relative location of the collapse mechanism lines, $V(V_u)$ and $Y(Y_u)$, and an elastic linear solution (see **Fig.4**). This is equivalent to the change in the combination of cross-sectional and material properties of Sec.1 and Sec.2. The yielding occurs initially at Sec.2 for the columns, C4-C6 and C9-C11, and at Sec.1 for C7-C8 and C12 (See **Table 2**). In the numerical analysis, at first the absolute maximum sway displacement is set as δ_y and then increased by 0.5δ_y every cycle.

(1) Load - displacement curves and sway displacement modes of columns

Fig.14 shows the sway displacement modes and load - displacement curves of columns C4-C8 with k of 0.2, 0.4 and 0.6. The squash force ratio is 0.5.

As is seen from figures (a) and (c), in accordance with the change in k of 0.2 to 0.6, the location corresponding to fixed end deflection moves from the bot-

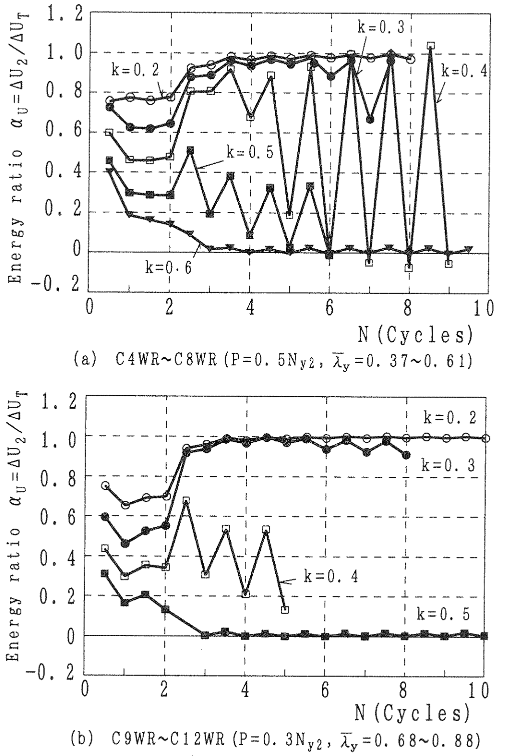

Fig.15 Variation of incremental energy absorbed by Sec.2 with number of cycles (E_t=0.01E)

tom of Sec.2 to Sec.1. The upper bounds of their resulting H - δ curves are mechanism lines Y_u and V_u, respectively. In the case of k=0.4, the displacement mode becomes antisymmetric for N≥5 and two collapse modes appear in a cycle by turns. The column C6 therefore exists in the transition region of collapse modes for the tip displacements assumed in this analysis. Since the column C6 has bending and buckling strengths greater than those of C4 (See **Table 2**), it is noted that the change of collapse modes is not concerned with the ultimate strength of the columns.

(2) Variation of absorbed energy ratio α_U

Fig.15 shows the variation of absorbed energy ratio α_U given by Eq.(8) for the columns C4-C12.

In the case of columns with k of 0.3, 0.4 and 0.5, α_U varies significantly when N≥7, 4 and 2.5, respectively. The collapse modes then begin to change every half cycle. The column C11 with k=0.4 and P/N_{y2}=0.3 also tends to show the same kind of behavior for N≥3.

(3) Discussion on hysteretic behavior of columns with variable cross-section

The phenomenon in which the collapse modes vary every half cycle is accompanied by a remarkable change in the peak loads, change in size and movement of hysteresis loops. Once it appears, these characteristics become significant, and hence this phenomenon should be classified as a nonstationary instability phenomenon of columns under cyclic loading.

When considering columns with variable cross-section in general steel frames designed rationally under working loads, they are found to have two or more collapse modes which simultaneously appear within the response near the linear elastic solution (see **Fig.4**). In this case, it is very important to know whether or not the instability phenomenon mentioned above appears in the inelastic hysteretic behavior of columns. It is then necessary to predict probable collapse mechanisms and to consider cyclic effects, such as the development of uniaxial strain, as well as the accumulation of residual deformation. These effects are highly related to the number of cycles, the magnitude and symmetry of applied displacement amplitude and squash force ratio. There is also need to investigate the effects of local buckling of plate elements on the collapse modes for columns with variable cross-section.

6. CONCLUSIONS

The elasto-plastic hysteretic behavior of cantilever columns with variable cross-section is presented in this paper.

The main conclusions obtained from this paper can be summarized as follows;

1) The columns with variable cross-section may show elasto-plastic behavior in which the collapse modes vary every half cycle accompanied by a change in plastic deformed portions.
2) This phenomenon is mainly due to $P\Delta$ effect caused by the accumulated residual curvature at the locations of column base and change in cross-section.
3) The resulting displacement mode of the columns is S shaped.
4) The corresponding load - displacement hysteresis loops have characteristics such that the peak loads decrease and increase in the regions of collapse modes Y and V, respectively, and hysteresis loops move gradually.
5) This behavior is an instability phenomenon of columns under cyclic loading which cannot be predicted through the overall buckling and bending strengths of columns.
6) The transition region where the collapse modes

change alternately is related to the location of change in cross-section.

7) It is necessary to experimentally confirm this instability phenomenon of columns with variable cross-section and to investigate the transition regions of collapse modes.

ACKNOWLEDGMENT: This research was partially supported by a 1990 grant from Daido Institute of Technology (DIT). The author wishes to thank Professors Hisao Kotoguchi and Tomisaku Mizusawa of DIT for their encouragement through this research. The author would also like to appreciate to Dr. J. Owen of University of Nottingham for correcting the draft in English of this paper.

REFERENCES

1) Nakai, H., Kawai, A., Kitada, T., Yoshikawa, O. and Miki, T.: A Survey on Steel Piers, *Bridge and Foundation Engineering*, Vol.16, No.6, June 1982, pp.35-40, Vol.16, No.7, July 1982, pp.43- 49.

2) Wakabayashi, M., Matsui, C. and et al.: Experimental Studies on the Elastic-Plastic Stability of Steel Frames (Part 1-4), *Proc. of Architectural Institute of Japan,* Part 1: No.192, pp.11-22, Feb. 1972, Part 2: No.193, pp.17-28, March 1972, Part 3: No.194, pp.9-20, April 1972 and Part 4: No.195, pp.25-38, May 1972.

3) Igarashi, T., Matsui, C., Yoshimura, K. and Matsumura, K.: Inelastic Behaviors of Structural Steel Sections under Alternative Loading - 2, Final State of Resisting Moment and Experimental Study, *Proc. of Architectural Institute of Japan*, No.170, pp.39-50, April 1970.

4) Matsui C. and Mitani, I.: Inelastic Behavior of High Strength Steel Frames Subjected to Constant Vertical and Alternating Horizontal Loads, *Proc. of Architectural Institute of Japan*, No.250, pp.31-41, Feb. 1976.

5) Wakabayashi M.: *Detailed Explanation of Theory for Structural Steel Frames*, Maruzen Co.Ltd., May 1985.

6) Nakamura, T. and Uetani, K.: Symmetry Limit Curves and Design Fundamental Curve for Cantilever Beam-Columns Subjected to cyclic reversed plastic bending, *Prof. of Architectural Institute of Japan,* No,346, pp.78-90, Dec.1984.

7) Nakai, H., Miki, T. and Ohgaki, K.: An Analytical Method for Critical Strength of Thin-Walled Steel Frames, *Memoirs of the Faculty of Engineering,* Vol.26, *Osaka City University*, pp.233-250, Dec.1985.

8) Crisfield, M.A.: An Arc-Length Method Including Line Searches and Accelerations, *International Journal for Numerical Methods in Engineering*, Vol.19, pp.1269-1289, 1983.

9) Japanese Road Association*: Specification for Highway Bridges*, Feb. 1991.

10) SSRC: *Guide to Stability Design Criteria for Metal Structures*, 4th Edition, Edited by Galambos, T.V., John & Wiley Sons, pp.57-66, 1988.